Letter

Laser-scribed graphene electrodes for aptamer-based biosensing

Christoph Fenzl, Pranati Nayak, Thomas Hirsch, Otto S. Wolfbeis, Husam Niman Alshareef, and Antje J Baeumner

ACS Sens., **Just Accepted Manuscript** • Publication Date (Web): 25 Apr 2017

Laser-scribed graphene electrodes for aptamer-based biosensing

Christoph Fenzl,[a] Pranati Nayak,[b] Thomas Hirsch,[a] Otto S. Wolfbeis,[a] Husam N. Alshareef,[b] and Antje J. Baeumner*,[a]

[a] Institute of Analytical Chemistry, Chemo- and Biosensors, University of Regensburg, Universitaetsstr. 31, 93053 Regensburg, Germany

[b] Materials Science & Engineering, King Abdullah University of Science & Technology (KAUST), Thuwal 23955-6900, Saudi Arabia

KEYWORDS: Laser-scribed graphene, biosensor, carbon nanomaterial, aptamer, immobilization, electrochemistry

ABSTRACT: Graphene as transducer material has produced some of the best-performing sensing approaches to date opening the door toward integrated miniaturized all-carbon point-of-care devices. Addressing this opportunity, laser-scribed graphene (LSG) electrodes are demonstrated here as highly sensitive and reliable biosensor transducers in blood serum analysis. These flexible electrodes with large electrochemical surface areas were fabricated using a direct-write laser process on polyimide foils. A universal immobilization approach is established by anchoring 1-pyrenebutyric acid to the graphene and subsequently covalently attaching an aptamer against the coagulation factor thrombin as an exemplary bioreceptor to the carboxyl groups. The resulting biosensor displays extremely low detection limits of 1 pM in buffer and 5 pM in the complex matrix of serum.

Numerous functional carbon materials have been investigated as electrodes for the detection of (bio)chemical analytes in electrochemical assays.[1–4] The electroanalytical performance of these materials is strongly influenced by the structural properties of the carbon itself which is mainly attributed to the density of electronic states as well as the edge-plane sites available on the surface.[5,6] Of all carbon materials, graphene has emerged as the most promising candidate.[7-9] Its water-dispersible derivatives, such as graphene oxide, are often used for the modification of electrodes but even when reduced through (physico)chemical means[10-12] the outstanding electrochemical properties of pristine graphene cannot be achieved due to numerous structural defects in graphene oxides.[13] To bridge the existing gap between lab research and commercial graphene-based biosensors, reliable, scalable fabrication and modification methods are still needed.[14] Here, standalone graphene electrodes can be a promising solution. El-Kady *et al.*[15] have introduced a novel and straightforward method to produce supercapacitors made of graphene by the direct laser reduction of graphene oxide with a standard LightScribe DVD optical drive. The resulting films – referred to as laser-scribed graphene (LSG) – show high electrical conductivity and specific surface area, are mechanically robust, and can be used directly as capacitor electrodes without the need of additives. In a following study,[16] Strong *et al.* built a low-cost graphene-based NO_2 gas sensor besting conventional carbon electrodes due to the LSG's superior electrical conductivity. Further, LSG can be easily printed, scaled, and is flexible.[17,18] For a broad range of biosensing applications, the high electron transfer rates, small peak potential differences and a good peak current response observed,[8,15,16] are extremely interesting. This includes, but not limited to, complex clinical diagnostics and implantable sensing arrays. LSG offers the possibility to create flexible, all-printed and implantable microarrays of electrodes with high surface area for the detection of multiple analytes such as biomarkers,[19] neurotransmitters,[20] proteins or other biomolecules.[21] To move LSG into the arena of biosensing, a reliable route for its modification with various biorecognition elements is required.[22] Here we demonstrate a universal modification route for LSG electrodes by anchoring 1-pyrenebutyric acid (PBA) via π-stacking and hydrophobic interactions to the LSG and subsequently covalently attaching bioreceptors to the carboxyl groups using standard coupling chemistry. An LSG-based electrochemical biosensor for thrombin (Figure 1) was developed to prove the viability of this strategy, as fast responding and miniaturized sensors for thrombin are urgently needed in point-of care diagnostics in order to replace existing and rather complex sensors and methods.

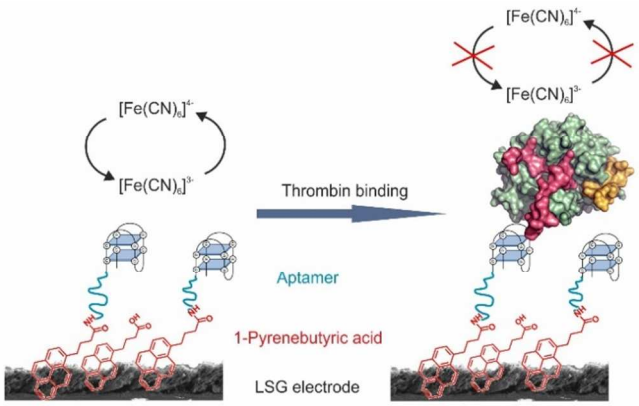

Figure 1. Schematic of the electrochemical thrombin detection mechanism. With increasing concentrations of thrombin, the diffusion of the redox marker hexacyanoferrate(III) to the electrode surface is increasingly hindered. This effect decreases the peak currents obtained from voltammetric measurements.

Laser-scribed graphene compares favorably to other carbon devices with respect to combining high electron transfer rates, small peak potential differences and a good peak current response with fast and scalable fabrication.[7,16] As it doesn't require fabrication masks or elaborate lithography equipment, which is the case for screen-printed electrodes and most microfabricated electrochemical biosensors, respectively, it is a highly attractive choice for electrochemical sensing (Figure 2).

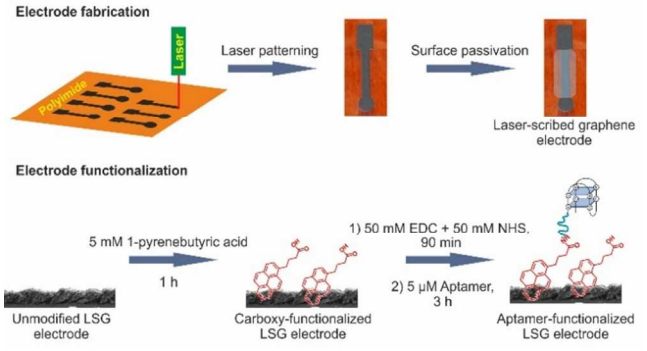

Figure 2. Electrode fabrication and functionalization process.

Scanning electron micrographs of the top-view of the electrode (Figure 3a and 3b) display a highly structured graphene film inscribed onto the polyimide foil with a large surface area. The cross-sectional view of the LSG electrode (Figure 3c) gives access to the sheet-like structure of the graphene layers with an average thickness of 35 µm.

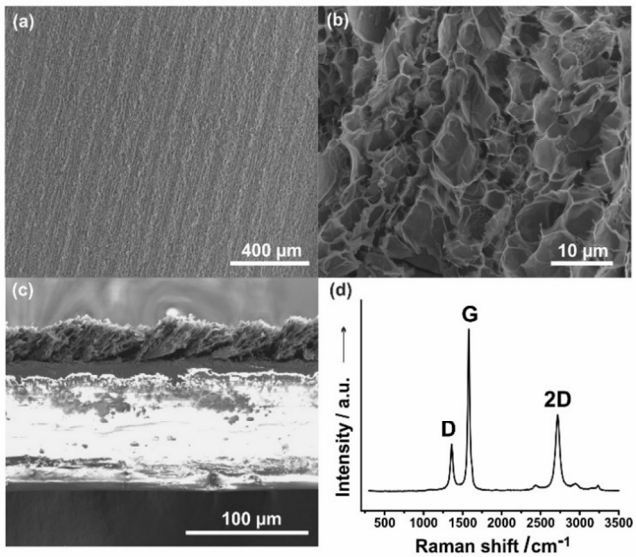

Figure 3. Characterization of the LSG electrodes. a,b) SEM images of the top view of the LSG electrode. c) cross-sectional SEM image of the same electrode. d) Raman spectrum of laser-scribed graphene.

Raman spectroscopy was used to prove the quality of the laser-scribed 2D-nanomaterial. Figure 3d shows the presence of the typical D, G and 2D peaks. The D peak at 1352 cm^{-1} suggests that there is a significant number of sp^3 centers present in the LSG due to structural edge defects. The prominent G band at 1584 cm^{-1} and the sharp 2D band at 2702 cm^{-1} further prove the presence of multi-layer graphene, as these bands are usually found at ~1580 cm^{-1} and ~2700 cm^{-1}, respectively. In contrast, the 2D peak of bulk graphite consists of two components.[23] The electrochemically active surface and the electron transfer rate of the LSG electrodes was determined using cyclic voltammetry (Figure 4a).

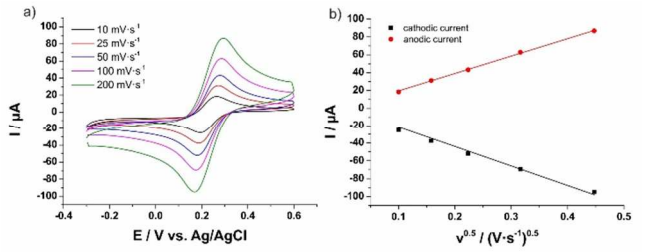

Figure 4. a) Cyclic voltammograms of LSG electrode vs. Ag/AgCl in PBS (at pH 7.4 containing 5 mM $K_3[Fe(CN)_6]$) at varying scan rates from 10 to 200 $mV \cdot s^{-1}$. b) Randles-Sevcik plot of LSG electrode vs. Ag/AgCl in PBS at pH 7.4 containing 5 mM $K_3[Fe(CN)_6]$ at varying scan rates from 10 to 200 $mV \cdot s^{-1}$.

The electrochemically active graphene surface area determined by the Randles-Sevcik plot (Figure 4b) is 1.3 ± 0.2 cm^2, which is more than 18-fold the physical area (0.07 cm^2) and is due to the lamella-like structure of the LSG (Figure 3a-c). The electron transfer rate (k^0) of LSG in phosphate buffered saline (PBS, pH 7.4) containing 5 mM $K_3[Fe(CN)_6]$ was calculated with an extended method of the Nicholson treatment[24] to be $k^0 = 0.0044 \pm 0.0003$ $cm \cdot s^{-1}$. This exceeds the k^0 of other carbon materials such as edge-plane (0.002601 $cm \cdot s^{-1}$) or basal-plane pyrolytic graphite (0.00033 $cm \cdot s^{-1}$). Using more complicated fabrication procedures, the k^0 can even be further increased as shown by Griffiths *et al.* (k^0 = 0.02373 $cm \cdot s^{-1}$), but comes at the cost of an additional drop coating step with graphene oxide prior to laser-scribing.[6]

Initial studies of the modification protocol revealed that pristine LSG does not possess enough functional groups for adequate immobilization of anti-thrombin aptamer (Figure 5a). For modification of the LSG electrodes with biorecognition molecules the graphene surface was modified with 1-pyrenebutyric acid via π-stacking interactions. This renders the electrode surface to bear a large number of COOH-groups available for rapid and gentle covalent coupling to amino-functionalized biorecognition elements such as the aptamer (Figure 2). The consecutive functionalization steps

were monitored via differential pulse voltammetry and can be seen in Figure 5b.

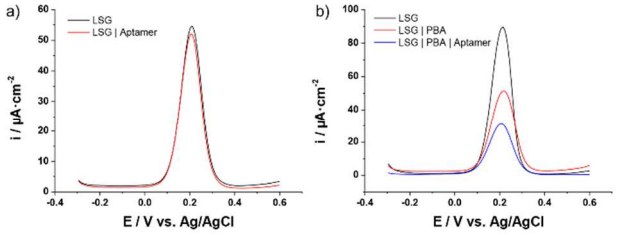

Figure 5. Differential pulse voltammograms of a LSG electrode without 1-pyrenebutyric acid (PBA) modification a) and after modification with PBA b) in PBS at pH 7.4 containing 5 mM $K_3[Fe(CN)_6]$ before and after attachment of anti-thrombin aptamer. In a) the peak current density drops only 4.7±0.4% due to insufficient functionalization with the aptamer. In contrast in b) the peak current density drops to 34.2±0.4% demonstrating the efficiency of PBA for modifications of LSG-electrodes.

Starting with the bare LSG electrode, the peak current of the unmodified electrode is as high as 130 µA due to an unhindered diffusion of the redox marker hexacyanoferrate(II/III) to the electrode surface. Upon addition of the first layer consisting of 1-pyrenebutyric acid, the peak current decreases to 57.5 ± 0.2% of the original value of non-modified LSG. After coupling of the amino-functionalized anti-thrombin aptamers to the carboxyl groups, the peak current further decreases to 34.2 ± 0.4% indicating the successful modification of the laser-scribed graphene electrode with the biorecognition elements.

In order to quantify the thrombin sensing properties of such modified LSG electrodes, the device was immersed into PBS containing thrombin in varying concentrations from 1 to 100 pM. Equilibration time was found to be at an optimum at 30 min which is faster than comparable approaches using redox-tagged aptamers[23] or an impedimetric sensing scheme.[26] After rinsing the electrode with PBS, it was placed in the electrochemical cell for DPV measurements. As expected, upon binding of thrombin to the aptamers, the available electrode surface for the redox marker is reduced resulting in decreasing DPV peak currents upon increasing thrombin concentrations. Thrombin binding to the LSG electrodes shows a saturation behavior common for antigen-antibody or antigen-aptamer interactions. Using the logarithmic concentration scale (Figure 6a), the DPV peak currents decrease linearly following the equation y = -33.9 - 2.41x, where y is the signal drop in $\mu A \cdot cm^{-2}$ and x is the logarithm of the thrombin concentration in $mol \cdot L^{-1}$ (R^2=0.97). Even a thrombin concentration as low as 1 $pmol \cdot L^{-1}$ results in a significant signal drop of -5.2 ± 0.3 $\mu A \cdot cm^{-2}$ increasing to -10.2 ± 0.6 $\mu A \cdot cm^{-2}$ at 100 pM thrombin.

With its low limit of detection (LOD) of 1 pM and its high sensitivity of -2.41 ± 0.16 $\mu A \cdot cm^{-2}$ per logarithmic concentration unit, this sensor is particularly useful when measuring pathological thrombin concentrations below the nanomolar level as found in healthy patients.[25] In fact, it compares favorably to the performance of other carbon-based thrombin sensing schemes with higher LODs (Table 1).[26–30]

Table 1. Comparison of different thrombin detection schemes.

Electrode material	Measurement method	Incubation time	Limit of detection	Interference studies	Reference
Reduced graphene oxide	Impedance spectroscopy	60 min	10 nM	In buffer	26
Pyrolyzed carbon	Impedance spectroscopy	15 min	0.5 nM	In buffer	27
Screen-printed carbon/AuNPs[a]	Stripping voltammetry	60 min	1 nM	In buffer	28
Reduced graphene oxide	Differential pulse voltammetry	20 min	0.45 fM	None	29
Gold	Differential pulse voltammetry	180 min	6.4 nM	In serum	30
Laser-scribed graphene	Differential pulse voltammetry	30 min	1 pM	In buffer and serum	This work

[a] Gold nanoparticles

Furthermore, aptamer-functionalized LSG excels at electrode-to-electrode reproducibility. The largest variation of four individual electrodes is 2.2% of the mean signal change at a thrombin concentration of 10 pM.

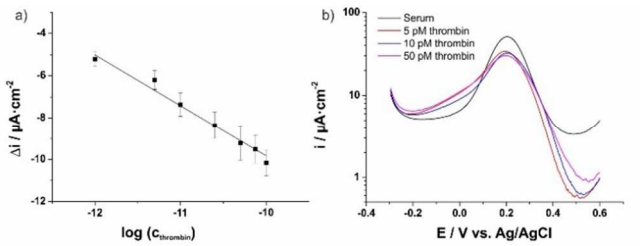

Figure 6. Change of the DPV peak current of PBA-modified LSG electrode after aptamer immobilization vs. Ag/AgCl at a) varying thrombin concentration and b) at varying thrombin concentration in serum. All measurements were conducted in phosphate buffered saline at pH 7.4 containing 5 mM $K_3[Fe(CN)_6]$. n=3.

The signal change of this sensing setup is based on the specific binding of thrombin to the immobilized aptamers and the resulting hindrance of diffusion of the redox marker. However, non-specific binding of interfering substances

such as other proteins can also impede this diffusion and thus lead to a decrease in the DPV peak current. Therefore, interference studies were performed with buffer containing bovine serum albumin (BSA) at a very high concentration of 40 g·L^{-1} and also with serum. After immersing the electrode into the solution for 30 min and rinsing with PBS, the DPV peak current drops significantly due to non-specific adhesion of BSA and serum proteins, respectively. Using these as blank values for the measurements with thrombin-spiked buffer with BSA and serum, increasing concentrations of thrombin correlated to the expected decreasing DPV peak currents (Figure 6b). The lowest detectable thrombin concentration in both cases is as low as 5 pmol·L^{-1} which is similar to the LOD in pure buffer. Also, in comparison to the measurements in PBS, both calibration curves show no deterioration of the sensitivity. In contrast, sensitivity is slightly increasing to -3.9 ± 0.3 μA·cm^{-2} per logarithmic concentration unit for the PBS with 40 g·L^{-1} BSA (Figure 7a) due to BSA's stabilizing effects on thrombin and is then decreasing again to -2.48 ± 0.04 μA·cm^{-2} per logarithmic concentration unit in presence of the numerous interfering substances present in serum (Figure 7b). This shows the high robustness of aptamer-modified laser-scribed graphene as sensor material in biomolecule detection.

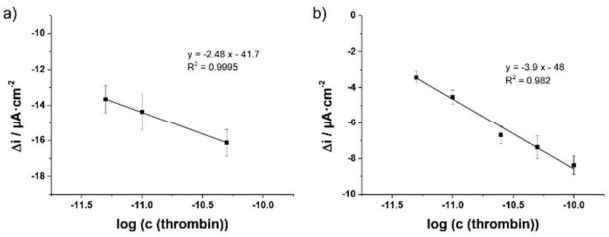

Figure 7. a) Change of the DPV peak current in PBS at pH 7.4 containing 5 mM $K_3[Fe(CN)_6]$ of 1-pyrenebutyric acid-modified LSG electrode after aptamer immobilization vs. Ag/AgCl at varying thrombin concentration in serum a) and in at varying thrombin concentration in PBS containing 40 g·L^{-1} bovine serum albumin b). n=3.

In conclusion, we have demonstrated the outstanding capabilities of directly-printed LSG electrodes to serve as electrochemical transducer in complex bioanalytical sensing environments. Our approach offers a combination of simple and scalable electrode fabrication of high-quality graphene, and a universal surface functionalization route with aptamers using PBA due to the 3D interconnected self-supporting network of LSG. Any biorecognition element can easily be immobilized on its surface and quantitative and sensitive detection is possible even in the most complex matrices such as serum. We believe that LSG has the capability to advance clinical diagnostics through miniaturized all-carbon electrode microarrays, flexible, implantable diagnostic tools, and multiplexed analysis.

EXPERIMENTAL SECTION

Materials: The polyimide foil for the LSG electrodes was purchased at Dasom RMS Co. LTD (Seoul, South Korea). 1-Pyrenebutyric acid, 1-ethyl-3-(3-dimethylaminopropyl)carbodiimide, N-hydroxysuccinimide, thrombin and fetal calf serum were obtained from Sigma-Aldrich (Taufkirchen, Germany). Anti-thrombin aptamer (5'-H_2N-C6-GGTTGGTGTGGTTGG-3') was purchased from Eurofins Genomics (Ebersberg, Germany). All other chemicals were obtained from VWR International (Darmstadt, Germany) and were of analytical grade.

Electrode Fabrication: The working electrodes (3 mm diameter) were printed on an X-660 laser cutter platform (Universal Laser Systems, Scottsdale, AZ, USA) with a wavelength of 10.6 μm. The optimized laser power, speed, pulses per inch (PPI) and the Z-distance between laser and the sample were 0.81 W, 5.8 cm·s^{-1}, 1000 PPI and 2 mm, respectively. All of the laser scribing experiments were performed under ambient conditions.

Electrode Characterization: The scanning electron microscope (SEM) images were recorded on a JSM-6510 scanning electron microscope (JEOL GmbH, Freising, Germany) at 10 kV. Raman microscopy was performed on a DXR Raman microscope (Thermo Fisher Scientific GmbH, Dreieich, Germany) at 532 nm laser excitation (10 mW).

Electrode Modification: First, LSG electrodes were modified with 5 mM 1-pyrenebutyric acid in DMSO for 60 min. Further, the electrodes were immersed in an aqueous solution 50 mM EDC and 50 mM NHS for 90 min followed by 1 μM anti-thrombin aptamer (5'-H_2N-C6-GGTTGGTGTGGTTGG-3') in an aqueous solution consisting of 100 mM NaCl and 4 mM EDTA for 3 h. The electrodes were extensively rinsed with phosphate buffered saline (PBS, pH 7.4).

Electrochemical characterization. This was performed using a CHI 650A Electrochemical Analyzer (CH Instruments, Austin, TX). A Pt wire counter electrode, Ag/AgCl reference electrode, and the respective working electrode were inserted into a 10 mL three-necked round-bottom flask and a solution volume of 7 mL was used for the measurements. The electrochemical measurements of the LSG electrode was performed in phosphate-buffered saline (PBS) containing 137 mM NaCl, 2.7 mM KCl, 10 mM Na_2HPO_4 and 1.8 mM KH_2PO_4 as well as 5 mM of the redox marker $K_3[Fe(CN)_6]$. The pH was adjusted to 7.4. Cyclic voltammograms were recorded from -0.3 V to 0.6 V with varying scan rates from 10 mV·s^{-1} to 200 mV·s^{-1}.

Electrochemical Thrombin Detection: The aptamer-modified LSG electrode was immersed into PBS containing thrombin at concentrations from 1 to 100 pM for 30 min. After rinsing with PBS, DPV measurements were performed with a potential ranging from -0.3 and 0.6 V vs. Ag/AgCl with a pulse width of 0.2 s and an amplitude of 50 mV. For the interference studies, bovine serum albumin was solved in PBS in a concentration of 40 g·L^{-1}. The electrode was immersed into this solution containing thrombin at concentrations from 0 (blank) to 100 pM for 30 min. After rinsing with PBS, DPV

measurements were again performed with a potential ranging from -0.3 and 0.6 V vs. Ag/AgCl with a pulse width of 0.2 s and an amplitude of 50 mV. As real samples, fetal calf serum was used. The electrode was immersed into the serum containing thrombin at concentrations from 0 (blank) to 100 pM for 30 min. After rinsing with PBS, DPV measurements were performed with the same adjustments as described above.

AUTHOR INFORMATION

Corresponding Author

*Email: antje.baeumner@ur.de

ACKNOWLEDGMENT

Research reported in this publication was supported in part by research funding from King Abdullah University of Science and Technology (KAUST).

REFERENCES

(1) Taleat, Z.; Khoshroo, A.; Mazloum-Ardakani, M. Screen-printed electrodes for biosensing: a review (2008–2013), *Microchim Acta* **2014**, *181* (9–10), 865–891.

(2) Ndamanisha, J. C.; Guo, L. Ordered mesoporous carbon for electrochemical sensing: A review, *Analytica Chimica Acta* **2012**, *747*, 19–28.

(3) Gan, T.; Hu, S. Electrochemical sensors based on graphene materials, *Microchim Acta* **2011**, *175* (1–2), 1. doi:10.1007/s00604-011-0639-7

(4) Loo, A. H.; Bonanni, A.; Pumera, M. Mycotoxin Aptasensing Amplificationbyusing Inherently Electroactive Graphene-Oxide Nanoplatelet Labels, *ChemElectroChem.* **2015**, *2*, 743–747.

(5) McCreery, R. L.; McDermott, M. T. Comment on Electrochemical Kinetics at Ordered Graphite Electrodes, *Anal. Chem.* **2012**, *84* (5), 2602–2605.

(6) Griffiths, K.; Dale, C.; Hedley, J.; Kowal, M. D.; Kaner, R. B.; Keegan, N. Laser-scribed graphene presents an opportunity to print a new generation of disposable electrochemical sensors, *Nanoscale* **2014**, *6* (22), 13613–13622.

(7) Joshi, R. K.; Alwarappan, S.; Yoshimura, M.; Sahajwalla, V.; Nishina, Y. Graphene oxide: the new membrane material, *Appl. Mater. Today* **2015**, *1*, 1–12.

(8) Shao, Y.; Wang, J.; Wu, H.; Liu, J.; Aksay, I. A.; Lin, Y. Graphene Based Electrochemical Sensors and Biosensors: A Review. *Electroanalysis* **2010**, *22* (10), 1027–1036.

(9) Eigler, S.; Hirsch, A. Chemistry with Graphene and Graphene Oxide—Challenges for Synthetic Chemists, *Angew. Chem. Int. Ed.* **2014**, *53* (30), 7720–7738.

(10) Zöpfl, A.; Sisakthi, M.; Eroms, J.; Matysik, F.-M.; Strunk, C.; Hirsch, T. Signal enhancement in amperometric peroxide detection by using graphene materials with low number of defects, *Microchim Acta* **2016**, *183*, 83–90. doi:10.1007/s00604-015-1600-y

(11) Kang, X.; Wang, J.; Wu, H.; Aksay, I. A.; Liu, J.; Lin, Y. Glucose Oxidase–graphene–chitosan modified electrode for direct electrochemistry and glucose sensing, *Biosensors and Bioelectronics* **2009**, *25* (4), 901–905.

(12) Wang, X.; Kholmanov, I.; Chou, H.; Ruoff, R. S. Simultaneous Electrochemical Reduction and Delamination of Graphene Oxide Films, *ACS Nano* **2015**, *9* (9), 8737–8743.

(13) Ratinac, K. R.; Yang, W.; Gooding, J. J.; Thordarson, P.; Braet, F. Graphene and Related Materials in Electrochemical Sensing, *Electroanalysis* **2011**, *23* (4), 803–826.

(14) Ito, Y.; Tanabe, Y.; Qiu, H.-J.; Sugawara, K.; Heguri, S.; Tu, N. H.; Huynh, K. K.; Fujita, T.; Takahashi, T.; Tanigaki, K.; Chen, M. High-Quality Three-Dimensional Nanoporous Graphene, *Angew. Chem. Int. Ed.* **2014**, *53* (19), 4822–4826.

(15) El-Kady, M. F.; Strong, V.; Dubin, S.; Kaner, R. B. Laser Scribing of High-Performance and Flexible Graphene-Based Electrochemical Capacitors, *Science* **2012**, *335* (6074), 1326–1330.

(16) Strong, V.; Dubin, S.; El-Kady, M. F.; Lech, A.; Wang, Y.; Weiller, B. H.; Kaner, R. B. Patterning and Electronic Tuning of Laser Scribed Graphene for Flexible All-Carbon Devices, *ACS Nano* **2012**, *6* (2), 1395–1403.

(17) Tian, H.; Shu, Y.; Cui, Y.-L.; Mi, W.-T.; Yang, Y.; Xie, D.; Ren, T.-L. Scalable fabrication of high-performance and flexible graphene strain sensors, *Nanoscale* **2014**, *6* (2), 699–705.

(18) Lin, J.; Peng, Z.; Liu, Y.; Ruiz-Zepeda, F.; Ye, R.; Samuel, E. L. G.; Yacaman, M. J.; Yakobson, B. I.; Tour, J. M. Laser-induced porous graphene films from commercial polymers, *Nature Communications* **2014**, *5*, 5714. doi:10.1038/ncomms6714.

(19) Nayak, P.; Kurra, N.; Xia, C.; Alshareef, H. N. Highly Efficient Laser Scribed Graphene Electrodes for On-Chip Electrochemical Sensing Applications, *Adv. Electron. Mater.* **2016**, *2* (10). doi: 10.1002/aelm.201600185

(20) Sanghavi, B. J.; Wolfbeis, O. S.; Hirsch, T.; Swami, N. S. Nanomaterial-based electrochemical sensing of neurological drugs and neurotransmitters, *Microchim Acta* **2015**, *182*, 1–41. doi:10.1007/s00604-014-1308-4.

(21) Gupta, R. K.; Pandya, R.; Sieffert, T.; Meyyappan, M.; Koehne, J. E. Multiplexed electrochemical immunosensor for label-free detection of cardiac markers using a carbon nanofiber array chip, *Journal of Electroanalytical Chemistry* **2016**, *773*, 53–62.

(22) Criado, A.; Melchionna, M.; Marchesan, S.; Prato, M. The Covalent Functionalization of Graphene on Substrates, *Angew. Chem. Int. Ed.* **2015**, *54* (37), 10734–10750.

(23) Ferrari, A. C. Raman spectroscopy of graphene and graphite: Disorder, electron–phonon coupling, doping and nonadiabatic effects, *Solid State Communications* **2007**, *143* (1–2), 47–57.

(24) Lavagnini, I.; Antiochia, R.; Magno, F. An Extended Method for the Practical Evaluation of the Standard Rate Constant from Cyclic Voltammetric Data, *Electroanalysis* **2004**, *16* (6), 505–506.

(25) Xiao, Y.; Lubin, A. A.; Heeger, A. J.; Plaxco, K. W. Label-Free Electronic Detection of Thrombin in Blood Serum by Using an Aptamer-Based Sensor, *Angewandte Chemie* **2005**, *117* (34), 5592–5595.

(26) Loo, A. H.; Bonanni, A.; Pumera, M. Impedimetric thrombin aptasensor based on chemically modified graphenes, *Nanoscale* **2012**, *4* (1), 143–147.

(27) Lee, J. A.; Hwang, S.; Kwak, J.; Park, S. I.; Lee, S. S.; Lee, K.-C. An electrochemical impedance biosensor with aptamer-modified pyrolyzed carbon electrode for label-free protein detection, *Sensors and Actuators B: Chemical* **2008**, *129* (1), 372–379.

(28) Suprun, E.; Shumyantseva, V.; Bulko, T.; Rachmetova, S.; Rad'ko, S.; Bodoev, N.; Archakov, A. Au-nanoparticles as an electrochemical sensing platform for aptamer–thrombin interaction, *Biosensors and Bioelectronics* **2008**, *24* (4), 825–830.

(29) Wang, Y.; Xiao, Y.; Ma, X.; Li, N.; Yang, X. Label-free and sensitive thrombin sensing on a molecularly grafted aptamer on graphene, *Chem Commun* **2012**, *48* (5), 738–740.

(30) Xiao, Y.; Lubin, A. A.; Heeger, A. J.; Plaxco, K. W. Label-Free Electronic Detection of Thrombin in Blood Serum by Using an Aptamer-Based Sensor, *Angew. Chem.* **2005**, *117* (34), 5592–5595.

TOC graphic

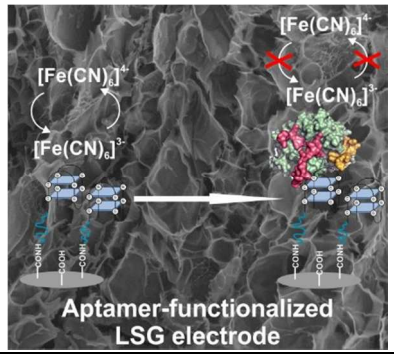
[Fe(CN)6]4-
[Fe(CN)6]3-
[Fe(CN)6]4-
[Fe(CN)6]3-
Aptamer-functionalized
LSG electrode